Experimental optimisation of waste-derived glycerol purification via electrodialysis under industrially relevant conditions

Taha Attarbachi [a,b], Kara Thomas [a], Martin Kingsley [b], Vincenzo Spallina [a,*]

[a] Department of Chemical Engineering, University of Manchester, M13 9PL, Manchester, United Kingdom
[b] Argent Energy Ltd., CH65 4BF, Ellesmere Port, United Kingdom

ARTICLE INFO

ABSTRACT

The purification of synthetic and pre-treated impure glycerol from 2nd generation biodiesel refineries is addressed to reduce the ash content below 1 % wt. Electrodialysis purification has been selected for its ability to selectively remove salts from the glycerol. First, synthetic glycerol-rich samples are tested to optimise cell voltage, membrane type and time on stream to achieve the target of 1 % wt. ash. After that, industrial pre-treated glycerol is used as a feed stream and compared. The comprehensive testing campaign demonstrated a recovery greater than 60 % with a glycerol purity greater than 82.2 % (wet and 90.4 % wt. dry basis) and ash content below 1 % wt. for 130–280 min and specific energy consumption ranging from 4.5 to 8.9 MWh•m^{-3} depending on the sample and conditions. to further decreases the ash content (below 0.5 % wt. corresponding to conductivity <2 mS•cm^{-1}) the energy requirement increases by almost three times confirming that while electrodialysis is a suitable technology for deeper waste stream purification, but energy supply and costs may hamper the implementation at scale.

List of Abbreviations and Definitions

Abbreviations	Definition
ACS	American Chemical Society
AEM	Anion Exchange Membrane
CEM	Cation Exchange Membrane
ANOVA	Analysis of Variance
DC	Direct Current
d.p.	Decimal Places
AOCS	American Oil 'Chemists' Society
ED	Electrodialysis
BS	British Standard
CAGR	Compound Annual Growth Rate
DF	Degree of Freedom
DOE	Design of Experiment
FAME	Fatty Acid Methyl Ester
FFA	Free Fatty Acids
FOG	Fats, Oils and Greases
HPLC	High-performance liquid chromatography
ICP-OES	Inductively coupled plasma–optical emission spectrometry
MONG	Matter Organic Non-Glycerol
OFAT	One Factor at a Time
PAC	Powdered Activated Carbon
POME	Palm Oil Mill Effluent
RID	Refractive Index Detector

(continued on next column)

(continued)

RSM	Response Surface Methodology
TAG	Triacylglyceride
UCO	Used Cooking Oil

1. Introduction

The European Union dictates a 14 % share of biofuels in the transportation sector in their Renewable Energy Directive EC/2009/28 for the year 2030 [1]. Among different options, the global biodiesel industry has grown from 1 million in 2008 to 40 million tonnes per year in 2023 [2]. A major by-product of biodiesel production is crude glycerol with 10 % wt. Therefore, up to 6.3 million tonnes of glycerol are expected by 2025 of which more than 10 % will be generated from 2nd generation biodiesel refineries using waste-feedstocks such as animal fats, FOGs (fats, oils, and greases) or UCO (used cooking oil) [2] which contain several impurities and are categorised as high-risk products and often disposed at cost. The use of this glycerol would require a high level of purification, typically by using vacuum distillation [3] which exhibits high CAPEX and high energy requirements. The typical composition of

* Corresponding author.
  E-mail address: vincenzo.spallina@manchester.ac.uk (V. Spallina).

crude glycerol from edible oil feedstock in comparison to the composition derived from waste-based feedstock produced by Argent Energy Group is depicted in Table 1.

Several alternatives have been considered for the highly impure glycerol purification that are promising for generating glycerol as raw feedstock for added value chemicals energy and fuel applications [2,6, 7]. Among different options, in the presence of highly polluted feedstock, physio-chemical purification has shown good results in reducing the ash content for bulk removal (up to 6–8%), however this would not make glycerol suitable for catalytic processes, such as reforming, liquid fuel conversion [8,9] and green fuel production [10]. This is associated with the limited glycerol-to-product conversion, inorganic solid handling, and catalyst deactivation as in the case of Ni-based for the reforming in presence of inorganic compounds.

Electrodialysis is a method used to reduce the ionic components of a mixture by applying a voltage and thus generating an electric field, which separates ions from the mixture using ion-exchange membranes. Electrodialysis has been proposed and widely studied for the desalination and purification of different streams [11] such as water and wastewater [12], metal recovery and removal [13] thus also providing answers to existing industrial challenges [14] in key sectors.

The principle of purification is explained by the salt and water fluxes that are generated across the membranes, as defined in equations (1) and (2), respectively.

$$J_s = J_{s,mig} + J_{s,diff} \tag{1}$$

$$J_w = J_{w,eo} + J_{w,os} \tag{2}$$

In these equations, J_s and J_w are defined as the salt (eq•m^{-2}•s^{-1}) and water flux (m^3•m^{-2}•s^{-1}), respectively. The salt transfer consists mainly of diffusion $J_{s,diff}$ and electromigration $J_{s,mig}$ while the water transfer consists of osmosis $J_{w,os}$ and electroosmosis $J_{w,eo}$ which takes place when ions drag water molecules with them once an electric field is applied as in the case of electrodialysis. When organic compounds are involved during the desalination such as during the desalination of crude glycerol (as in the case of MONG) a third equation (3) must be considered.

$$J_o = J_{o,diff} + J_{o,mig} \tag{3}$$

$J_{o,diff}$ is the total diffusion flux (organic acid molecules and organic acid ions) while $J_{o,mig}$ is the total migration flux (convection of organic acid molecules and electromigration of organic acid ions). Further explanations and elaborations for these equations can be found in Liu et al. [15] and Han et al. [16] who investigated the effect of electrodialysis on organic solutes during desalination.

Different authors have investigated the reduction of ash content from glycerol mixtures using electrodialysis by using commercial membranes (Table 2) and using different glycerol sources. Rozhdestvenskaya et al., Schepper et al. and Vadthya et al. have all used synthetically prepared glycerol solutions with added salt [17–19] while Dzyazko et al. and Schaffner et al. have used glycerol from a biodiesel plant and a diester plant, respectively [20,21]. Schaffner et al. used a bipolar electrodialysis

Table 1
Typical crude glycerol composition derived from different feedstocks [4,5].

Composition	Palm Oil	Argent Energy
Glycerol [% wt.]	53.19 ± 0.77	51.36 ± 8.71
Water [% wt.]	18.79 ± 0.11	22.85 ± 10.74
Ash [% wt.]	2.80 ± 0.10	10.57 ± 3.55
MONG [% wt.]	25.24 ± 0.97	15.22 ± 5.95

Table 2
Different research works on the purification of electrodialysis using glycerol as a starting material.

Author	Year	Membrane Type (manufacturer)	Starting Material	Main Outcome
Dzyazko et al. [20]	2017	Composite membranes CMI 7000 and AMI7000 (Membrane International)	Effluent Biodiesel production	Decrease of salt concentration by 100 times; modification increases stability against fouling
Rozhdestvenskaya et al. [17]	2017	Composite membranes CMI 7000 and AMI7000 (Membrane International)	Synthetic glycerol (90 % wt.) - water (10 % wt.) mixtures with NaCl (100–1500 mol•m^{-3}), process solution (1000 mol•m^{-3} NaCl) with 8 % wt. organic impurities	90 % desalination of solution, electrodialysis is only first stage of desalination, long resistance against poisoning by organic substances
Schaffner et al. [21]	2003	Bipolar membranes BP-1 ACM anionic membrane CMB cationic membrane (Tokuyama Soda)	By-product of diester plant (65 % glycerol on a dry basis)	80 % demineralisation rate, 95 % glycerol after concentration with less than 2 % mineral content, specific energy consumption: 0.5 kWh•kg^{-1}
Schepper et al. [18]	2019	FAB-FKB,FAM-FKM, FAS-FKS (Fumatech) AMX-CMX (Neosepta) MVA-MVK, SA-MV (PCA) AMC-CMH (Ralex)	Synthetic aqueous glycerol-containing mixture (NaCl)	low ratio glycerol/NaCl is desirable; the performance of ion-selective membranes for specific separations cannot be derived effectively from the typical membrane suppliers and literature
Vadthya et al. [19]	2015	CMI-7000 Ultrex AMI-7001 Ultrex (Membrane International)	Synthetic glycerol-water-salt mixtures	Successful removal of 95 % Na$_2$SO$_4$; membrane and energy cost of $0.09 per m^3 of feed processed for a production rate of 1 m^3•h^{-1}

membrane mode, while Dzyazko et al. mentioned a homogeneous ash content of 1000 mol•m^{-3} of NaCl. However, as the biofuel industry moves towards waste-based feedstocks due to criticism of using edible oils from crops, which compete with food prices, the resulting crude glycerol produced tends to contain a higher amount of impurities (among them ionic compounds), leading to higher complexity for the separation process. The main research novelty in this work is the use of

pre-treated, industrially derived, waste-based (crude) glycerol from biodiesel refineries that utilise exclusively waste-based feedstocks for their biodiesel production. This has a major impact on the purity of the yielded crude glycerol which is currently disposed at cost [2,22,23]. Furthermore, this research work focuses more on the industrial feasibility of the process as compared to existing research in this area, which focuses more on the fundamental transport principles in this system. This will give researchers and industrial stakeholders valuable insights into a sustainable solution for the purification of their waste-derived feedstock.

In this work, the starting material has been provided by a waste-based biodiesel manufacturer (Argent Energy Group). Their feedstock is currently being disposed of at cost and converted into biogas since the biodiesel is generated from free fatty acids, waste oils and fats, animal fat (tallow) or ABP of categories 1 and 2 which cannot be used for food or animal feed, used cooking oil (UCO), food waste (such as bakery wastes, contaminated sauces, condiments or oil extracted from food waste collection) and effluent ponds [24]. Given the legal and technical circumstances, the purified glycerol cannot be sold. Therefore an alternative purification route must be developed to recover the energy content of the glycerol and use it elsewhere. The industrial-derived glycerol used in this study has been previously treated via physio-chemical processes to reduce ashes from 16.1 to 8.6 % wt. and MONG from 25.6 % to 4.9 % wt. to make it suitable for the electrodialysis deep purification step [2,22,23]. Before testing this glycerol for the validation of the methodology, an experimental optimisation of the purification process has been carried out using a response surface methodology (RSM) using a synthetic mixture to assess the influence of stack voltage, type of membrane and initial salt content within a range of relevant operating conditions. The study primarily focuses on the definition of process standards that could provide real performance – valid for industrial applications and large scale – in terms of specific energy consumption [MWh•m^{-3}], glycerol recovery [%], cycle time [min] to reduce the ash content by assessing the change in conductivity via electrodialysis. Finally, given the relevance of membrane lifetime [25], the impact of fouling on performance decay and the characterisation of tested samples were compared in both synthetic and real mixtures.

This work aims to confirm and validate the electrodialysis process for waste recovery and valorisation. It is complementary to ongoing studies on the development of electrodialysis membranes and devices since it entails their application and performance from a process perspective. The novelty of the paper relies on methodology and results achieved and more specifically on: i) comprehensive testing and optimisation by response surface methodology (RSM) of electrodialysis process for glycerol at different ash levels to derive glycerol recovery and energy requirements; ii) validation of the optimised conditions with three different industrially-derived glycerol streams; iii) analysis of the membranes lifetime, the impact of glycerol initial composition and effect of regeneration on purification performance; iv) effect of water dilution to glycerol purity and separation time; v) quantitative assessment of cost escalation to achieve deep glycerol purity and iv) inform the industry on opportunities for the process scale up by operating the ED process over a wide range of industrially-relevant conditions.

2. Materials and methods

2.1. Glycerol feedstock

Two different crude glycerol samples from biodiesel plants were provided, namely STANLOW (1) and STANLOW (2). The waste glycerol by-products obtained are in both cases dark-brown, with a strong odour, however, STANLOW (2) has a low viscosity due to the existing high moisture content while STANLOW (1) has a high viscosity due to the comparably lower moisture content, making the handling of both raw materials slightly different; this is a stark contrast from the clear, colourless glycerol which can be obtained commercially or the light brown/yellow crude glycerol obtained from facilities that use exclusively UCO as feedstock because of impurities and MONG content (see Appendix 1).

Samples of 2000 g of crude glycerol were pre-treated using a sequence of physio-chemical techniques [18]. Three purified glycerol samples have been considered in this study as results of the treatment process, all industrially relevant given the source of the glycerol, referred to as 'Industrial Glycerol A', 'Industrial Glycerol B', 'Industrial Glycerol C', and 'Industrial Blend' which is a mixture of all samples after pre-treatment before being sent for the purification with ED. Finally, de-ionised water was added to each sample to use a standard 50 % wt. glycerol content in the ED unit. The composition of all samples is reported in Table 3 while the appearances are shown in Fig. 1.

To understand the performance of the ED unit against glycerol composition, the optimisation of the operating conditions was carried out using synthetic solutions with commercial pure glycerol, de-ionised water, and salt (NaCl) as in Table 4. Such decision is required to reduce the risk of membrane fouling, blocking and potentially irreparable damage during the process of screening and testing. The ash content range (5–15 % wt.) has been selected based on the average value of the industrial glycerol (Table 3). It must be noted that ash content is the largest difference between crude glycerol produced from waste-based

Table 3
Waste glycerol samples used in this work.

Composition t = 0	Glycerol [% wt.]	Ash [% wt.]	Water [% wt.]	MONG [% wt.]
STANLOW (1)	56.82	16.11	7.44	19.63
STANLOW (2)	44.23	12.19	33.17	10.41
Average	50.53 ± 6.30	14.15 ± 1.96	20.31 ± 12.87	15.02 ± 4.61
Industrial Glycerol A	72.40	8.29	3.32	15.99
Industrial Glycerol B	78.79	8.63	2.14	10.44
Industrial Glycerol C	78.01	8.94	3.99	9.06
Industrial Blend	77.68	8.71	2.84	10.77
Industrial Diluted				
Industrial Glycerol A	50	5.73	33.77	10.5
Industrial Glycerol B	50	5.47	38.73	5.8
Industrial Glycerol C	50	5.73	38.46	5.81
Industrial Blend	50	5.61	37.46	6.93

Fig. 1. Left: STANLOW (1), Middle: STANLOW (2), Right: Physio-chemically pre-treated glycerol samples.

Table 4
Synthetic aqueous glycerol solutions containing different amounts of salts for the design of experiment runs.

Composition	Synthetic Solution A	Synthetic Solutions B	Synthetic Solutions C
Glycerol [% wt.]	40.0	45.0	50.0
Ash [% wt.]	15.0	10.0	5.0
Water [% wt.]	45.0	45.0	45.0
MONG [% wt.]	–	–	–

feedstocks and first-generation oil feedstocks. Moreover, waste-based crude glycerol can contain varying amounts of ash accumulated from the acid and base catalysts used during the esterification/trans-esterification reactions and, as in the case of the glycerol samples from industry received in Manchester, from the addition of further chemicals and salts required to recover FFA, methanol and other relevant compounds from the glycerol-rich phase.

2.2. Experimental set-up

A three-chambered Micro BED System was used, which was made by PCCell GmbH (Heusweiler, Germany) [26]. The three chambers of this rig are referred to as the 'diluate', 'concentrate' and the 'electrolyte' with the respective pumps to keep the fluids in a closed loop. Due to the fact that the Micro BED ED system is solely used for testing the feasibility of electrodialysis applications, the pumps did not allow a variation of the flow rate. Hence, the nominal flow-through rate per cell was constant at 0.5 L•h^{-1}. Furthermore, the maximum applicable stack voltage was 22 V and the maximum amperage was 0.8 A. They are all connected to the cell which contains the membrane stack as shown in Fig. 2.

The diluate chamber contains the glycerol solution to be purified, and the concentrate chamber contains the solution which facilitates the purification by accumulating the ions removed from the diluate. The electrolyte chamber contains Na_2SO_4, which is required to maintain the 'electrodes' conductivities. The anolyte and catholyte chambers of the cell are connected via banana jacks to a DC power supply from VOLT-CRAFT (Type: PPS-16005), which applies a voltage and generates the electric field necessary to move charged ions.

Two different commercial homogeneous ion exchange membrane stacks were used (Supplementary Information Section 1). Both membrane stacks have an end spacer at either end of the ten cell pairs, and they are currently used in water purification.

2.3. Chemicals

The chemicals used in this experiment are summarised in (Supplementary Information Section 1). A 6–8 % wt. sodium sulphate (Na_2SO_4) was required as the electrolyte solution, which corresponds to a conductivity in the range of 50–80 mS cm^{-1}. A 10 % wt. nitric acid (HNO_3) solution was required to clean the membrane regularly and remove the organic fouling resulting from MONG and glycerol deposition.
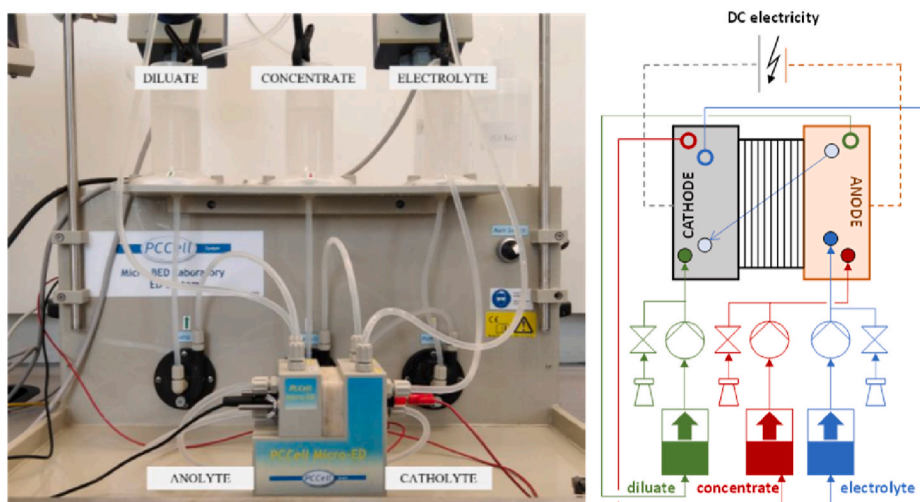

Fig. 2. Left: Electrodialysis rig set-up used for the study showing piping and connections with chambers for the desalination. Right: Schematic of Micro BED ED rig from PCCell.

Table 5

Summary of the design of experiments which has been used to set up experiments necessary to determine optimal conditions for electrodialysis.

Run	Voltage [V]	Initial Ash Content [% wt.]	Membrane
1	10	11.05	M1
3	22	15	M1
5	22	5	M1
6	22	10	M1
7	14.56	15	M1
9	16	5	M1
13	10	5	M1
14	16	10	M1
2	16	10	M2
4	16	10	M2
8	22	15	M2
10	22	5	M2
11	16	10	M2
12	10	5	M2
15	10	15	M2

2.4. Optimisation methods

A set of experiments were designed to determine the optimal conditions for electrodialysis. Stack voltage, ash content and membrane type were varied. Since the ED cell measures the conductivity of the diluate, each experiment was carried out by running the electrochemical purification until a final conductivity of 5 mS•cm^{-1} was achieved. The optimal conditions were dictated by response variables, which in this case were the energy consumption (lowest), the glycerol recovery (highest), and the separation cycle time (lowest). These response variables were selected given their relevance in the assessment of process feasibility since they indicate the energy demand, yield, size and footprint for a given feed flow rate and ash removal conditions. The design of experiments was created using JMP® which produced a set of 15 experiments to be conducted and listed in Table 5.

The minimum voltage was determined experimentally by carrying out tests with a solution of glycerol in the electrodialysis rig starting from 1 V and increasing to 1 V every 20 min until the mixture began to desalinate and decrease in conductivity. Once optimal conditions had been established with synthetic glycerol, pre-treated and industrially derived glycerol samples were used. The case of purified glycerol was selected to assess the impact of the membrane fouling in the presence of long-chain organic compounds (MONG). The runs were completed three times for each solution, and results were averaged to ensure repeatability.

The purification process is mainly done to remove ashes, while limiting glycerol losses from the diluate. Therefore, the glycerol recovery and ash removal have a significant influence on the feasibility and implementation of the process. Glycerol recovery was calculated with equation (4) using the mass of diluate at the inlet ($m_{dil,t=0}$) and outlet ($m_{dil,t=1}$) and the inlet and outlet glycerol concentrations ($w_{Gly,t=0}$, $w_{Gly,t=1}$). The ash removal was calculated according to equation (5) using the inlet and outlet ash contents ($w_{Ash,t=0}$, $w_{Ash,t=1}$). Hence equation (4) provides the performance of the purification process to avoid any losses (in the diluate) on the glycerol compound in the feed stream which is the key compound to desalinate, while equation (5) indicates the capacity of the electrodialysis unit to remove ashes (from the diluate) which are the main compounds to be removed from the feed stream. Energy consumption E was determined on a cumulative, specific basis in units of MWh•m^{-3}$_{DIL}$ using equation (6) where I is the current (A), U is the voltage (V), t is the time (min), and v_{dil} is the measured diluate volume (mL). It is important to mention that the specific energy consumption is based on the glycerol-water mixture left after the electrodialysis purification and not the only glycerol compound. The specific energy consumption was used to make the results of each experiment more comparable as the diluate solution decreased in volume during the run.

$$Y_{Glycerol} = \frac{m_{dil,t=1} \times w_{Gly,t=1}}{m_{dil,t=0} \times w_{Gly,t=0}} \quad (4)$$

$$R_{Ash} = 1 - \frac{m_{dil,t=1} \times w_{Ash,t=1}}{m_{dil,t=0} \times w_{Ash,t=0}} \quad (5)$$

$$E = \int_0^t \frac{I \times U \times dt}{v_{dil}} \approx \frac{I \times U \times \Delta t}{v_{dil}} \quad (6)$$

2.5. Analytical methods

2.5.1. Glycerol, ash, water, and MONG analysis

Glycerol content was analysed following BS 5711–3:1979 standards through titration against 0.1 M NaOH [27]. Ash content was determined following the BS 5711–3:1979 methodology by heating the sample so all that remains is the ash using a furnace (Nabertherm P300, Germany) [28]. This is achieved by weighing out 10 g of the sample into a crucible using a 4 d.p. (decimal places) mass balance. Water content is determined by following the standard method ISO 2097-1972 using a Karl-Fischer titration device (Metrohm 899 coulometer, Germany) [29]. A syringe is used to add a small sample to the titration device. All procedures are described in detail in the Supplementary Information (Section 2). After that, MONG content can be calculated according to equation (7).

$$MONG \text{ [% wt.]} = 100 - Glycerol \text{ [% wt.]} - Water \text{ [% wt.]} - Ash \text{ [% wt.]} \quad (7)$$

3. Results and discussion

3.1. Optimisation for synthetic glycerol solutions

The design of experiments was conducted initially with membrane M1, followed by membrane M2, to reduce the impact of changing the membrane. The results from the set of experiments are shown in Table 6, and they include the final glycerol and ash content, the experimental time, glycerol recovery and calculated energy consumption.

The final glycerol content in the H_2O-glycerol mixture results in 45.1 ± 6 % wt. with ash content of 0.92 ± 0.3 % wt. This consistency in the results demonstrates that both low and high ash content feedstock could yield similar final products. It must be noted that the glycerol recovery is primarily impacted by the secondary losses, e.g. leakages, crossovers or cell geometry, which heavily depends on membrane area [30]. This effect is limited when the process is operated at an industrial scale in larger devices.

Table 6

Results from the design of experiments and analysis conducted on recovered diluate solution.

| Run	Glycerol [% wt.]	Ash [% wt.]	Time [min]	Glycerol Recovery [%]	Energy Consumption [MWh•m^{-3}]
1	45.59	0.87	464	66.03	26.02
2	43.39	0.87	360	72.51	28.80
3	47.43	1.10	216	63.55	43.15
4	45.63	0.86	390	73.22	32.51
5	46.14	0.90	121	83.22	5.20
6	46.45	1.16	170	68.22	18.33
7	45.48	1.02	319	61.94	37.77
8	46.79	1.03	411	65.29	83.09
9	46.50	1.03	155	83.51	4.16
10	47.47	1.03	147	74.17	6.25
11	41.82	0.67	360	68.57	27.33
12	45.57	0.78	289	74.22	5.94
13	43.36	0.94	223	77.46	3.83
14	45.70	0.72	230	72.15	16.51
15	38.83	0.86	810	39.50	79.42
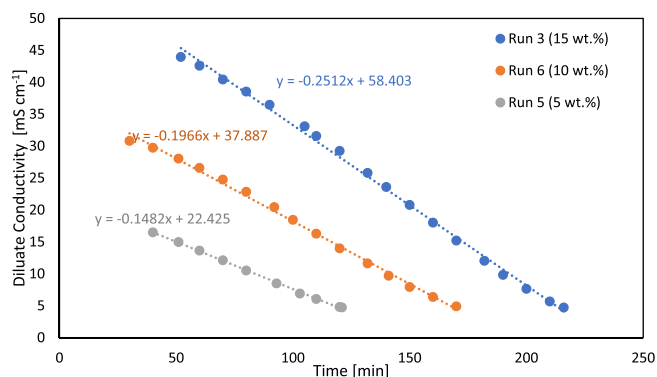
Fig. 3. Graph showing how desalination rate is impacted by ash content, with runs taking longer for higher ash contents but also having an increased rate of desalination (Membrane M1, Voltage 22 V). Table 5 provides the information on the run considered and Table 6 reports all results for the experimental campaign.
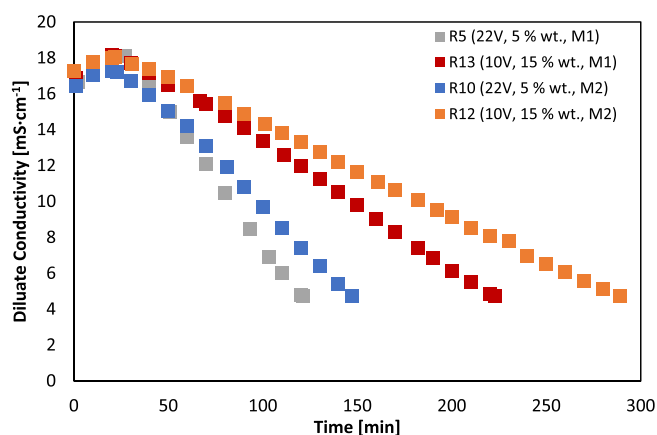

Fig. 4. Graph showing how increased voltage leads to an increased rate of desalination and decreased overall desalination time for M1 and M2. Table 5 provides the information on the run considered and Table 6 reports all results for the experimental campaign.

3.1.1. Impact of ash content

The time required to reach the target conductivity (5 mS cm^{-1}) increases with increased ash content. The ED unit could desalinate each sample to the same final point despite the significant changes in time required (Fig. 3). The first 20–40 min were not considered in the summary of the results due to the need to get a convergence of diluate and concentrate conductivity. After that, for all cases, the conductivity, hence the ash content, decreases linearly with time. A greater salt content increases the rate at which the solution desalinates, as it can be seen by the slope of the fitting curve reported in Fig. 3. As anticipated, the glycerol recovery does not change significantly. Instead, the energy required to complete the purification (which is impacted by the testing time) increases from 5.20 to 43.15 MWh m^{-3} when the initial ash content increases from 5 % wt. ash 15 % wt. ash (using M1 and stack voltage of 22 V).
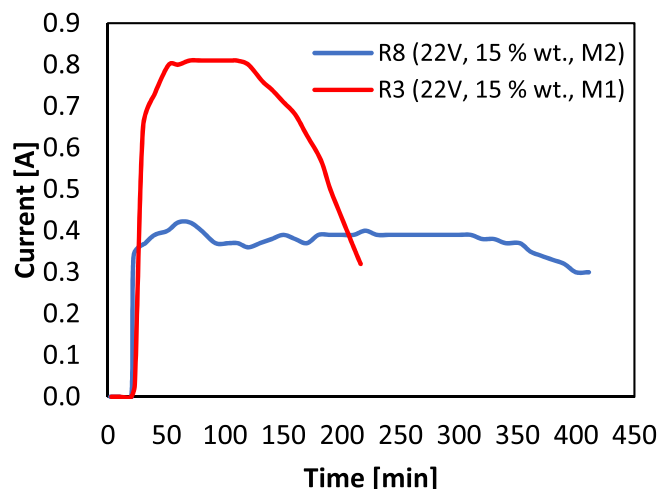

Fig. 5. Comparison of the effect M1 and M2 have on the current achieved during electrodialysis.
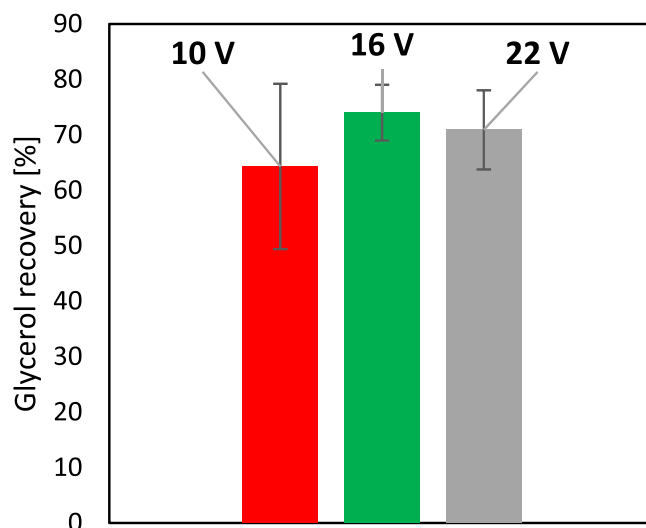

Fig. 6. Influence of different voltages on glycerol recovery.

3.1.2. Impact of voltage

Increasing stack voltage reduces the time to achieve the desired conductivity (Fig. 4). At lower voltage, the current density decreases, hence the ion flux, and therefore, the longer time required for ions to move across the membrane. Applying a higher voltage would also lead to a higher net force on ions in the electric field, yielding a transfer momentum to water and glycerol through viscous drag [31].

At the maximum stack voltage (22 V), the time for desalination changes greatly depending on the initial ash content (103–317 min), similarly for 10 V, with time greatly increased (219–675 min). Furthermore, the recovery improves with higher voltages because a lower cycle time decreases the accumulation of secondary losses: at 22 V, runs deliver an average glycerol recovery of 70.89 ± 7.14 %, while at 10 V the recovery is limited to 64.30 ± 14.91 %. At increased stack

voltage, the ED delivers more power, hence a larger unit cost in terms of capacity. However, the energy consumption also depends on the cycle time, which is more dominant at this scale. Thus, the total energy required increases from 6.29 to 12.34 MWh•m^{-3}.

3.1.3. Effect of type of membrane

Across all experiments, M1 appeared favourable to M2 with, on average, higher glycerol recoveries (+5.2 %), decreased specific energy consumptions (−50 %), and time on stream (−158 min) while achieving similar ash contents as depicted in (Fig A1 in the appendix). This is likely because M1 has a higher transference number, which impacts positively the removal of negatively charged anions (Cl-in this case) hence current, and they are able to move faster as in the case of M2, which is designed for standard water desalination application. Together with the lower resistance of the AEM, the membranes M1 can remove anions quicker than M2. It can be observed in Fig. 5 that the current for a solution of 15 % wt. ash at 22 V using M2 is much lower compared to M1; consequently, glycerol desalination takes longer.

3.1.4. Summary of optimised conditions

In Table 6 can be observed that the glycerol recovery is higher than 60 % for almost all of the runs except run 15 (long operating time). Part of the glycerol is lost to the concentrate solution as the polar glycerol molecules get pulled through the membrane with the free ions in the solution due to the electroosmotic drag, which was discussed earlier. The amount of glycerol lost during the experiments has an optimum at approximately 16 V, as shown in Fig. 6. This is explained by a greater driving force at increased voltage leading to more fluid and ionic transfer across the membrane, shorter cycle times, and higher losses due to the drag of fluids across the membrane. On the other hand, lower voltage implies a longer cycle time, which brings additional mass losses (via fluid transfer across the membrane) to the system, especially for those run with high ash content, i.e. an optimum of 16 V is very reasonable.

The average proportion of glycerol lost in the system across all 15 runs was 14.16 % ± 4.9 %, which is a substantial amount with glycerol recovery in the range of 60 %–85 % for most of the experiments. Further details on the system's mass balance are reported in the Supplementary Information (section 3).

Due to the batch nature of the experiments, the mass transfer between compartments is reduced while salts are separated from the diluate; this occurs because in a batch system, the concentration of salt in the diluate progressively reduces and it increases in the concentrated, hence the driving force that governs the diffusions is also reduced because the concentration difference across membrane tends to decrease. The analysis presented led to optimal conditions using the membrane M1 with the lower ash content of 5 % wt. at a voltage of 16.28 V (See Fig A2 in the Appendix). In such case, a cycle time of 120 min is expected with glycerol recovery of 84.7 % and energy consumption of 1.35 MWh•m^{-3}.

Once the optimal conditions were found, a final run was conducted, and the results obtained are shown in Table 7 (the run was conducted once). The time and energy consumption were as expected from the previously conducted experiments; however, the glycerol recovery was lower (71.4 %) than the predicted case (84.7 %). This is due to membrane usage (before rinsing or cleaning) over time and some damage associated with the switching of the membrane stack between M1 and

Table 7
Results obtained from electrodialysis conducted at optimal conditions obtained from prediction profile.

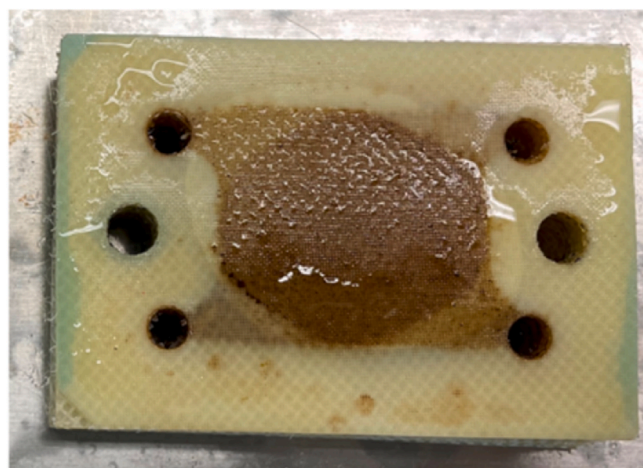|	Glycerol [% wt.]	Ash [% wt.]	Time [min]	Glycerol Recovery [%]	Energy Consumption [MWh•m^{-3}]
Optimal	43.56	0.89	136	71.41	4.51

Fig. 7. Spacers filled with hydrophobic, viscous content and hindering the flow of diluate.

Table 8
Summary of results for the industrial glycerol purified via electrodialysis, including averages vs the optimised synthetic glycerol run.

Run	Glycerol [% wt.]	Ash [% wt.]	Time [min]	Glycerol Recovery [%]	Specific Energy Consumption [MWh•m^{-3}]
Industrial Glycerol A	40.43 ± 1.20	1.32 ± 0.06	291 ± 17.93	66.55 ± 8.91	8.46 ± 0.62
Industrial Glycerol B	42.59 ± 0.76	1.23 ± 0.05	282 ± 18.93	67.24 ± 1.48	8.50 ± 0.99
Industrial Glycerol C	43.06 ± 1.06	1.46 ± 0.14	275 ± 20.22	52.91 ± 8.03	9.58 ± 0.65
Average Industrial	42.03 ± 1.15	1.34 ± 0.09	282.67 ± 6.55	62.23 ± 6.60	8.85 ± 0.52
Synthetic glycerol Optimised (Table 7)	43.56	0.89	136	71.41	4.51

M2 (micro-cracks on the membrane surface due to excess exchange of membranes). The recovery rate, ash removal and time required are relevant for industrial applications and technology development since they can provide input to the design of the process equipment, and costs associated with glycerol production and electric utility demand.

3.2. Testing of pre-treated industrial crude glycerol with the optimum conditions obtained from the design of experiment runs

Solutions were prepared using pre-treated, industrially derived glycerol, in which MONG is also present. The solutions were tested three times to improve the reliability of the results. A final test was conducted using a blend of 'Industrial Glycerol 'A', 'Industrial Glycerol 'B' and 'Industrial Glycerol 'C' '('Industrial 'BLEND') pushing the purification down to 2 mS•cm^{-1}. The overall mass balance and description of the physio-chemical purification process for each glycerol sample are reported in the Supplementary Information (section 4). Evidence of the presence of hydrophobic matter and the effect on the membrane are shown in Fig. 7. The accumulation of viscous, non-water-soluble matter in the membrane stack clearly reduces the active surface area and quickly hinders the flow of ions through the membrane. Such behaviour was not recorded in the previous campaign using synthetic glycerol. A summary of the purification results can be seen in Table 8, and the detailed results of each run are summarised in Supplementary
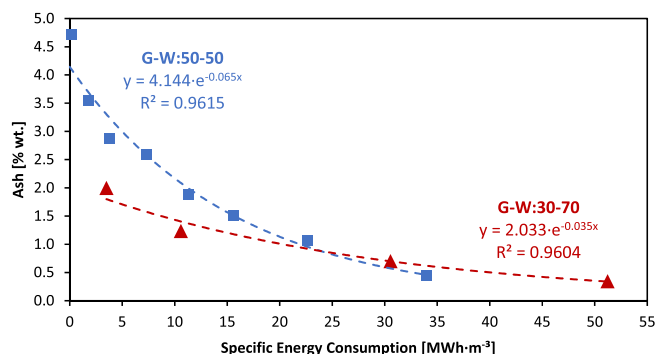
Fig. 8. Specific energy consumption [MWh•m^{-3}] in relation the ash content [% wt.] of the mixture with visual evolution of ash content from 10 mS cm^{-1} to 2 mS cm^{-1}.

Information (section 4).

The glycerol purity is almost similar for all industrial crude glycerol processes, with a total average of 42.03 ± 1.15 % wt. (rest is water and minor MONG). This result corroborates the previous evidence on synthetic glycerol purification carried out in section 3.1, showing that electrodialysis can render standard quality glycerol independently of the composition and source of the glycerol used. On a higher level, these results provide relevant information to the industry, which could confidently enable low-quality waste recovery and use for energy applications (e.g. glycerol-steam reforming [8,9] in the H2020 GLAMOUR project). These results also suggest that the purification approach based on physiochemical pre-treatment and deep purification with electrodialysis could be used for other feedstock from oleochemical, process wastewater, effluents from agriculture and biochemical processes.

However, some differences remain and they are associated with the ash content. Approximately twice the amount of ashes can be measured compared to the optimal synthetic glycerol run, although the same conductivity (5 mS•cm^{-1}) was measured in the diluate (average 1.34 % wt. with low standard deviation). Such difference may be due to ion competition in the presence of potassium (in particular), sodium, phosphorous and sulphuric components with an array of different minor other ionic compounds detected in the ICP-OES analysis of the final sample in Supplementary Information (Section 4) in contrast with synthetic glycerol, where only NaCl was used.

In terms of purification time, industrial-derived glycerol samples require about twice the time recorded with synthetic glycerol, which also reflects the energy consumption as per equation (6). The reasons for longer batch times using industrial glycerol are various, among them molecular size and shape leading to steric effects, hydration numbers of different ionic compounds and finally, the solute hydration effect [16]. Furthermore, organic molecules (MONG), especially with high hydrophilicity due to their functional groups such as –OH, are generally competing with inorganic ionic compounds as they can pass through the membrane easier due to the free volume of the membrane [32]. The difference in glycerol recovery between synthetic and industrial glycerol is 9.2 % (ranging from 2.6 % to 15.8 % including the level of uncertainties recorded by performing the experimental campaign). Since the main difference between the two cases is the time on stream to achieve the same final ash content, such difference corroborates the hypothesis on the impact of secondary losses.

'Industrial Glycerol C' shows a significant deviation in glycerol recovery compared to the other two industrial samples. However, these results were affected by the intermediate membrane cleaning to remove excess fouling, leading to free membrane volume and increased transfer.

Using the 'industrial BLEND glycerol', referred to as G-W:50-50 in Fig. 8, a final comparison has been carried out to achieve deep purification with a final diluate conductivity of 2 mS•cm^{-1}. This experiment
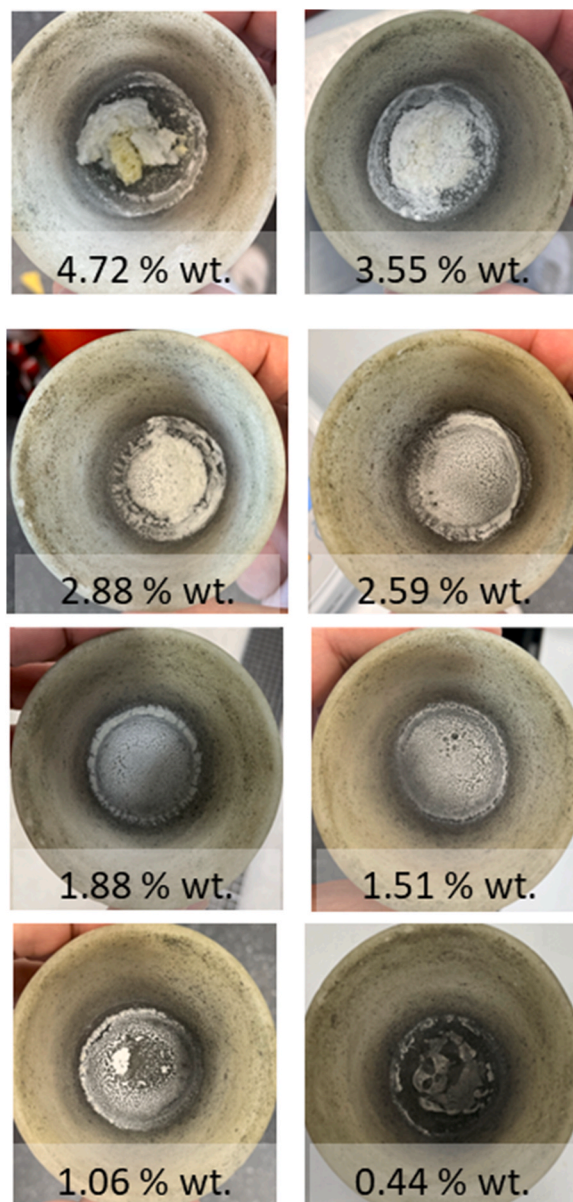

Fig. 9. Ash residues from the glycerol-rich stream after periodic sampling at different conductivities.

Table 9
Comparison between the BLEND trial and the averages and standard errors of industrial glycerol runs.

Run	Average A-B-C	BLEND
Glycerol [% wt.]	42.03 ± 1.15	43.83
Ash [% wt.]	1.34 ± 0.09	0.47
Time [min]	282.67 ± 6.55	636.00
Glycerol Recovery [%]	62.23 ± 6.60	82.24
Specific Energy Consumption [MWh•m^{-3}]	8.85 ± 0.52	34.03

consists of sampling the diluate periodically and measuring the ash content, and, at the same time, recording the resulting energy consumption to achieve such a level of purification. The initial ash content of 4.72 % wt. (corresponding to and 10 mS•cm^{-1} conductivity), was reduced to 0.44 % wt. (2 mS cm^{-1}). The same test was carried out with
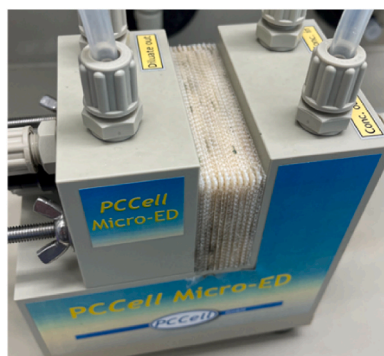
Fig. 10. Visible fouling in the membrane package which is placed in the cell.

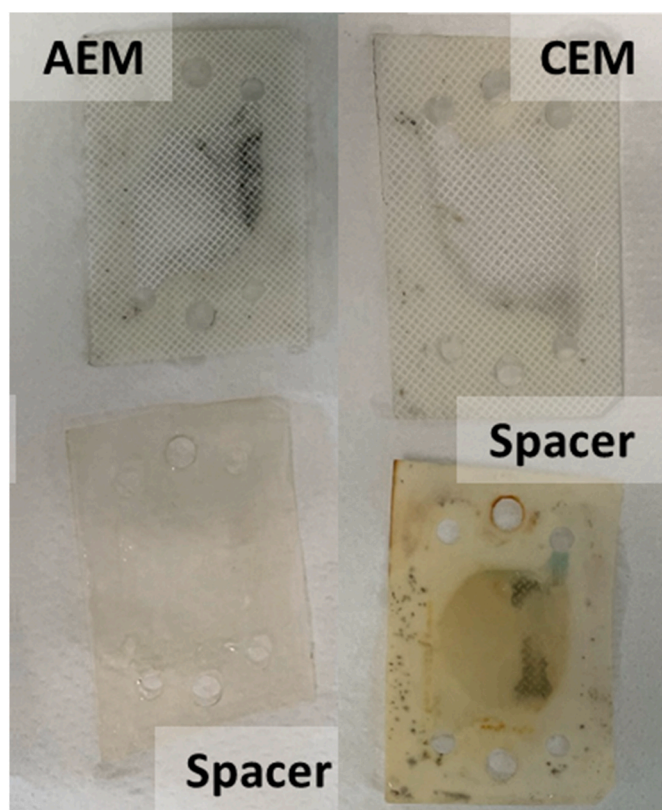**Fig. 11.** Impact of MONG of industrial glycerol on the electrodialysis membranes and spacers.
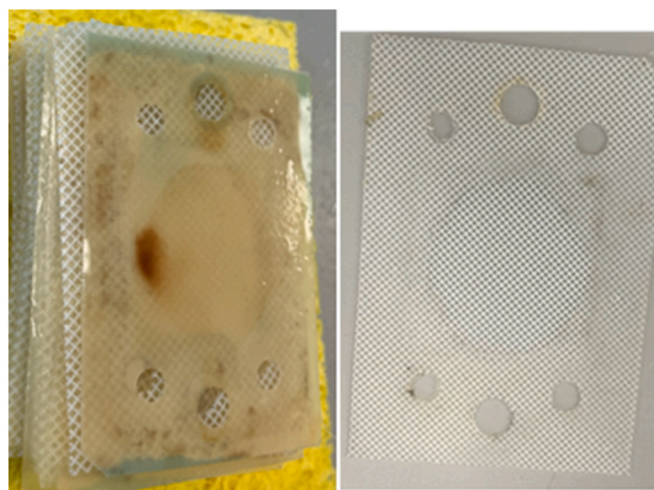

Fig. 12. AEM and spacer after treatment with nitric acid and sponge (mechanical cleaning).

glycerol-rich batch with low H_2O content would be less cost-intensive than the other case. However, the overall impact on the costs should also include the costs for glycerol pre-treatment (in G-W:50-50) and the costs of H_2O addition in (G-W:30–70), especially if a downstream process does not tolerate/require H_2O in its feed.

The solid residues associated with the amount of ashes in glycerol can be seen in Fig. 9.

Table 9 confirms that the glycerol purity achieved is slightly higher due to the reduction in ash content for the test with blended glycerol (BLEND) compared to the average results of the three separate cases (average A-B-C). Nevertheless, the results also show a significant increase in specific energy consumption ($\times$ 3.85 times) to reduce the ash content below 1 % wt. despite the marginal increase in glycerol recovery. The reason for this is the reduction of the conductivity in the diluate compartment over time, making it necessary to maintain a high driving force across the membrane to remove residual ions.

3.2.1. Membrane fouling

Membrane fouling has been observed in this work from the start of the trials using industrial glycerol, as can be seen in Figs. 10, 11 and 12 for the disassembled stack after using industrial glycerol. Black dots on the AEM clearly show the impact of MONG content while CEM remains clear, proving that naturally occurring MONG content is generally negatively charged and impacts AEM more than CEM, as shown already in different research works [33].).

While several positive effects were recorded after membrane cleaning, glycerol recovery dropped by approximately 20 % (74.87 %–54.74 %). After further trials, the recovery increased back to over 75 %, and after further cleaning, the recovery was limited to 59.9 %. Glycerol recovery is therefore strongly dependent on membrane flux which reduces in the presence of fouling. Fouling reduces the separation of the ions through the membrane, thus limiting the separation rate and eventually causing an increase in glycerol secondary losses because of a longer time on stream to achieve the same level of purity.

The detailed characterisation of the membrane would require further study/analysis to discriminate and quantify its performance and

crude glycerol from the biodiesel refinery (without physio-chemical conditioning as in other cases discussed in this section) with a single centrifugation step to remove non-polar impurities and diluted with de-ionised water down to 30 % wt. glycerol (referred to as G-W:30–70 in Fig. 8). From this comparison, it can be concluded that to achieve the same amount of ashes in the diluate compartment, higher water content is more beneficial in terms of energy consumption up to a threshold of slightly below 1 % wt. (intersection of curves). After that, operating a

optimisation to increase lifetime, flux and stability. Given the cost of the part considered, the limited availability of the membrane stack in combination with the need to carry out more experimental testing, an in-depth analysis of the fouling mechanism has not been considered in this study and the analysis has been focused only at the macroscopic level.

4. Conclusion

The electrodialysis process has been extensively presented and demonstrated as a purification technique to achieve a high level of glycerol purification from industrially derived samples.

For synthetic glycerol, the optimal conditions have been established of 16.3 V, 5 % wt. and using a thinner membrane, which exhibits low resistivity. The optimal conditions were also tested and validated in pre-treated industrial glycerol samples with marginal differences in the ash content and glycerol purity, while significant deviations were observed in terms of purification time and, consequently, specific energy consumption. An ultra-low desalination test to achieve 2 mS cm^{-1} of conductivity was proven as technically feasible, with a glycerol recovery of over 80 %.

Future works require a rigorous techno-economic assessment to establish if the process is also viable along with scale-up, tuning and optimisation of the ED process for the specific application as well as some improvements on other conditions such as water/glycerol ratios and glycerol pre-treatment. The process optimisation would require more detailed characterisation to explain the interactions between MONG/ashes with membranes in order to correlate the type of membrane with lifetime and minimise the need for cleaning or replacement. Moreover, the validity of the process implemented, which includes a mild glycerol pre-treatment can be used for different feedstocks.

Therefore, similar studies could focus on organic wastes to further enhance waste recovery and multi-feedstock bio-based refinery, which would certainly impact the biomass supply chain and, ultimately, the achievement of ambitious targets for biofuel and biochemical production.

CRediT authorship contribution statement

Data availability

Data will be made available on request.

Acknowledgements

Appendix A. Supplementary data

Supplementary data to this article can be found online at https://doi.org/10.1016/j.biombioe.2024.107334.

Appendix

A1: GCMS MONG analysis of a random sample (conducted by Argent Energy Group).

Table 10
GCMS MONG analysis of a sample, conducted by Argent Energy Group

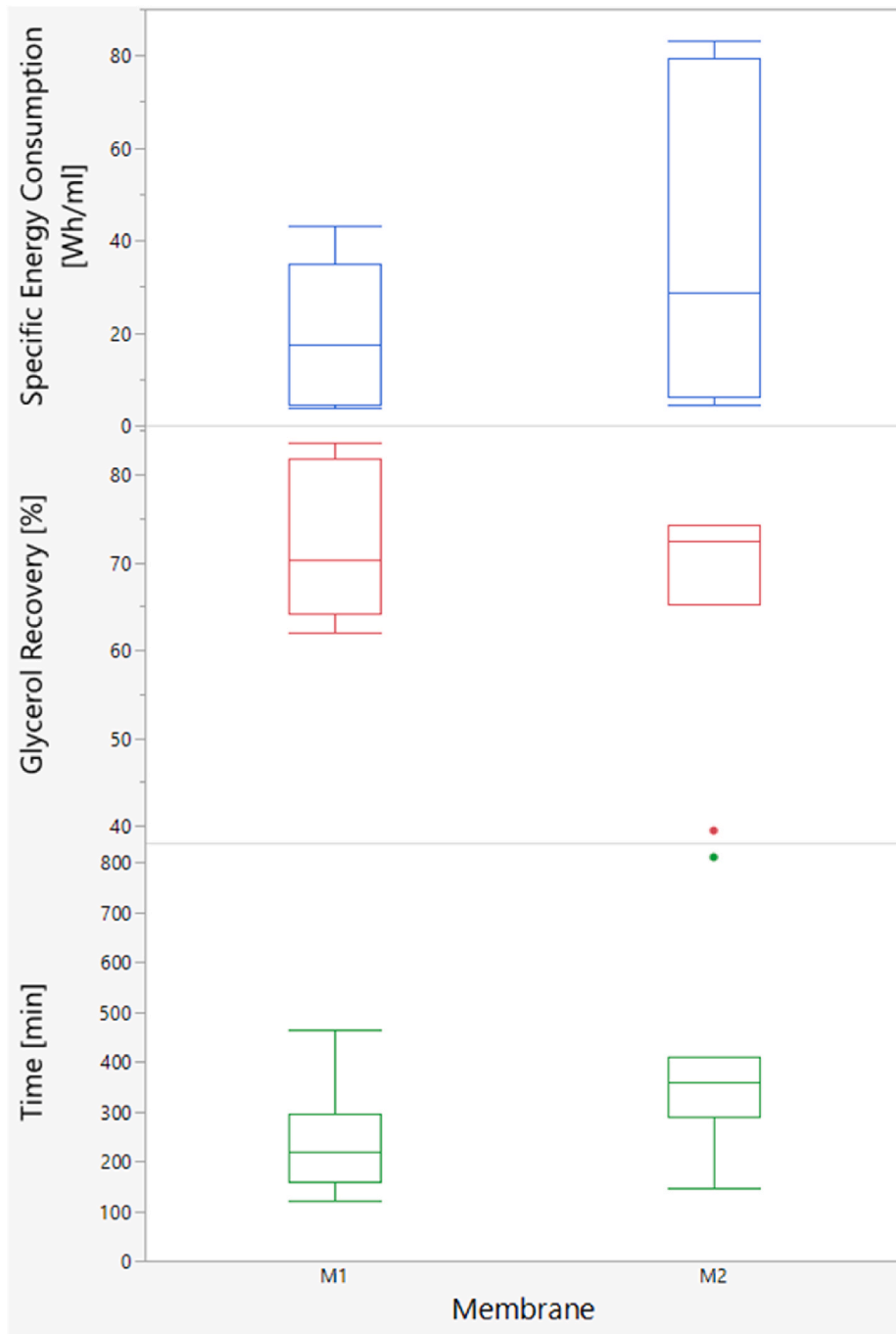| Fraction	% wt.
Short chain acids	23.1
Long chain acids	3.8
FAME	16.9
Other	9.4

Fig. A1. Impact of 'Membrane Type' M1 and M2 on 'Glycerol Recovery', 'Specific Energy Consumption' and 'Time'. Figure generated with JMP®.
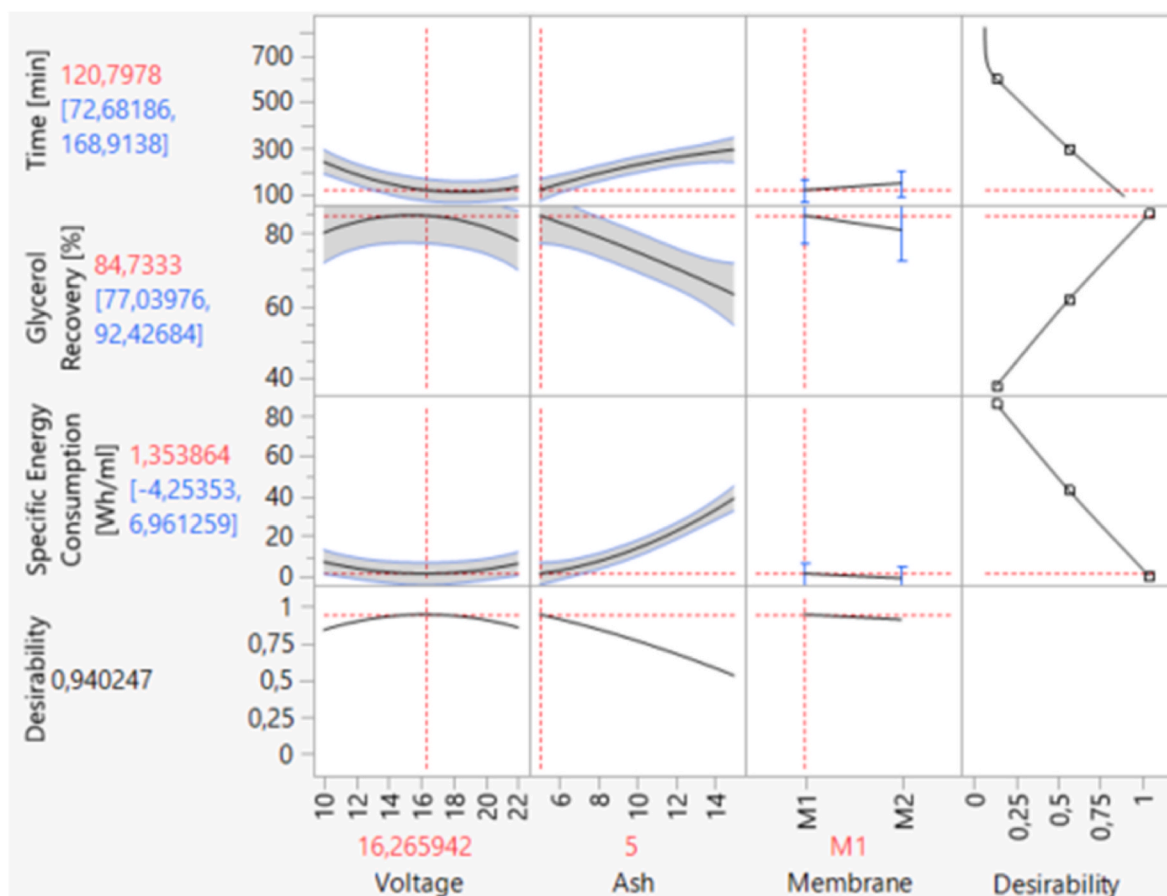
Fig. A2. Prediction profile produced as a result of the design of experiments conducted showing the optimal voltage of 16.27 V for solutions containing 5 % wt. ash and desalinated using M1. Figure generated with JMP®.

References

[1] M. Schöpe, Renewable energy directive, Eur. Wind Energy Conf. Exhib. 1 (2008) 32–38.

[2] T. Attarbachi, M.D. Kingsley, V. Spallina, New trends on crude glycerol purification: a review, Fuel 340 (2023) 127485, https://doi.org/10.1016/j.fuel.2023.127485.

[3] M.S. Ardi, M.K. Aroua, N.A. Hashim, Progress, prospect and challenges in glycerol purification process: a review, Renew. Sustain. Energy Rev. 42 (2015) 1164–1173, https://doi.org/10.1016/j.rser.2014.10.091.

[4] A.H.N. Armylisas, S.S. Hoong, T.N.M. Tuan Ismail, Characterization of crude glycerol and glycerol pitch from palm-based residual biomass, Biomass Convers. Biorefinery (2023), https://doi.org/10.1007/s13399-023-04003-4.

[5] T. Attarbachi, M. Kingsley, V. Spallina, Experimental scale-up and technoeconomic assessment of low-grade glycerol purification from waste-based biorefinery, Ind. Eng. Chem. Res. 63 (2024) 4905–4917, https://doi.org/10.1021/acs.iecr.3c03868.

[6] S. Kongjao, S. Damronglerd, Purification of crude glycerol derived from waste used-oil methyl ester plant, Kor. J. Chem. Eng. 27 (2010) 944–949, https://doi.org/10.1007/s11814-010-0148-0.

[7] R. Manosak, S. Limpattayanate, M. Hunsom, Sequential-refining of crude glycerol derived from waste used-oil methyl ester plant via a combined process of chemical and adsorption, Fuel Process. Technol. 92 (2011) 92–99, https://doi.org/10.1016/j.fuproc.2010.09.002.

[8] J.M. Silva, L.S. Ribeiro, J.J.M. Órfão, M.A. Soria, L.M. Madeira, Low temperature glycerol steam reforming over a Rh-based catalyst combined with oxidative regeneration, Int. J. Hydrogen Energy 44 (2019) 2461–2473, https://doi.org/10.1016/j.ijhydene.2018.11.234.

[9] C. de Leeuwe, S.Z. Abbas, A. Amieiro, S. Poulston, V. Spallina, Carbon-neutral and carbon-negative chemical looping processes using glycerol and methane as feedstock, Fuel 353 (2023) 129001, https://doi.org/10.1016/j.fuel.2023.129001.

[10] A. Sandid, T. Attarbachi, R. Navarro-Tovar, M. Pérez-Page, V. Spallina, J. Esteban, Production of triacetin from industrially derived purified glycerol: experimental proof of concept, kinetic model derivation and validation, Chem. Eng. J. 496 (2024), https://doi.org/10.1016/j.cej.2024.153905.

[11] T. Xu, C. Huang, Electrodialysis-based separation technologies: a critical review, Am. Inst. Chem. Eng. AIChE J. 54 (2008) 3147–3159, https://doi.org/10.1002/aic.11643.

[12] S. Al-Amshawee, M.Y.B.M. Yunus, A.A.M. Azoddein, D.G. Hassell, I.H. Dakhil, H. A. Hasan, Electrodialysis desalination for water and wastewater: a review, Chem. Eng. J. 380 (2020), https://doi.org/10.1016/j.cej.2019.122231.

[13] J.M. Arana Juve, F.M.S. Christensen, Y. Wang, Z. Wei, Electrodialysis for metal removal and recovery: a review, Chem. Eng. J. 435 (2022) 134857, https://doi.org/10.1016/j.cej.2022.134857.

[14] A. Cournoyer, L. Bazinet, Electrodialysis processes an answer to industrial sustainability: toward the concept of eco-circular economy?—a review, Membranes 13 (2023), https://doi.org/10.3390/membranes13020205.

[15] J. Liu, J. Liang, X. Feng, W. Cui, H. Deng, Z. Ji, Y. Zhao, X. Guo, J. Yuan, Effects of inorganic ions on the transfer of weak organic acids and their salts in electrodialysis process, J. Membr. Sci. 624 (2021) 119109, https://doi.org/10.1016/j.memsci.2021.119109.

[16] L. Han, S. Galier, H. Roux-de Balmann, Transfer of neutral organic solutes during desalination by electrodialysis: influence of the salt composition, J. Membr. Sci. 511 (2016) 207–218, https://doi.org/10.1016/j.memsci.2016.03.053.

[17] L.M. Rozhdestvenskaya, Y.S. Dzyazko, E.O. Kudelko, S.L. Vasilyuk, V.N. Belyakov, Desalination of glycerol-water solutions by electrodialysis using the organo-inorganic membranes, J. Water Chem. Technol. 39 (2017) 26–32, https://doi.org/10.3103/S1063455X17010052.

[18] W. De Schepper, M.D. Moraru, B. Jacobs, M. Oudshoorn, J. Helsen, Separation and Purification Technology Electrodialysis of aqueous NaCl-glycerol solutions: a phenomenological comparison of various ion exchange membranes, Sep. Purif. Technol. 217 (2019) 274–283, https://doi.org/10.1016/j.seppur.2019.02.030.

[19] P. Vadthya, A. Kumari, C. Sumana, S. Sridhar, Electrodialysis aided desalination of crude glycerol in the production of biodiesel from oil feed stock, Desalination 362 (2015) 133–140, https://doi.org/10.1016/j.desal.2015.02.001.

[20] Y.S. Dzyazko, L.M. Rozhdestvenska, S.L. Vasilyuk, K.O. Kudelko, V.N. Belyakov, Composite membranes containing nanoparticles of inorganic ion exchangers for electrodialytic desalination of glycerol, Nanoscale Res. Lett. 12 (2017), https://doi.org/10.1186/s11671-017-2208-4.

[21] F. Schaffner, P.Y. Pontalier, V. Sanchez, F. Lutin, Bipolar electrodialysis for glycerin production from diester wastes, Filtr. Sep. 40 (2003) 35–39, https://doi.org/10.1016/S0015-1882(03)00037-5.

[22] T. Attarbachi, M. Kingsley, V. Spallina, Waste-derived low-grade glycerol purification and recovery from biorefineries: an experimental investigation, Biofuels, Bioprod. Biorefining (2024), https://doi.org/10.1002/bbb.2638.

[23] T. Attarbachi, M. Kingsley, V. Spallina, Experimental scale-up and technoeconomic assessment of low-grade glycerol purification from waste-based biorefinery, Ind. Eng. Chem. Res. (2023), https://doi.org/10.1021/acs.iecr.3c03868.

[24] Biodiesel | Argent Energy, (n.d.). https://www.argentenergy.com/what-we-do/our-biodiesel/(accessed August 3, 2023).

[25] W. Guo, H.H. Ngo, J. Li, A mini-review on membrane fouling, Bioresour. Technol. 122 (2012) 27–34, https://doi.org/10.1016/j.biortech.2012.04.089.

[26] Electrodialysis Systems and Ion Exchange Membranes - PCCell GmbH, (n.d.). https://www.pccell.de/en/P160-Industrial-scale-system_18_content2_Pilot-Units_82_Produktdetail.html (accessed February 21, 2022).

[27] B. Standard, Sampling and Test for Glycerol, 1979.

[28] B. Standard, Sampling and Test for Glycerol — Ash, 1979.

[29] K. Fischer, Sampling and Test for Glycerol — Part 8 : Determination of Water Content, 1979.

[30] E. Cell, E. Sandoval-s, Z. De, M. Miranda-hern, E. Mendoza, Effect of Gaskets Geometry on the Performance of a Reverse, 2022, pp. 1–11.

[31] D. Wiley, G. Fimbres Weihs, Electroosmotic drag in membranes, Encycl. Membr. (2016) 653–654, https://doi.org/10.1007/978-3-662-44324-8_2078.

[32] Z. Qiao, Z. Wang, C. Zhang, S. Yuan, Y. Zhu, J. Wang, PVAm–PIP/PS composite membrane with high performance for CO_2/N_2 separation, AIChE J. 59 (2012) 215–228, https://doi.org/10.1002/aic.

[33] V. Lindstrand, A.S. Jönsson, G. Sundström, Organic fouling of electrodialysis membranes with and without applied voltage, Desalination 130 (2000) 73–84, https://doi.org/10.1016/S0011-9164(00)00075-8.